
Research Paper

Novel Film Modifiers to Alter the Physical Properties of Composite Ethylcellulose Films

Lai Wah Chan,¹ Kang Teng Ong,¹ and Paul Wan Sia Heng^{1,2}

Received October 18, 2004; accepted December 6, 2004

Purpose. Polyvinylpyrrolidone (PVP), molecular-composite PVP, and Plasdene S-630 copolyvidonum are potential polymeric film modifiers for achieving improved drug release. The aim of this study was to investigate how these polymeric additives would affect the physicomechanical properties of composite ethylcellulose films.

Methods. The miscibility of these polymeric additives with ethylcellulose was determined from the differential scanning calorimetry (DSC) thermograms of various polymer blends formed from organic solvents. It was found that ethylcellulose (EC) was miscible with the polymeric additives up to a concentration of 50%. Ten percent to 30% w/w polymeric additives were then added to aqueous ethylcellulose dispersion to form composite films. The morphology, film transparency, dynamic mechanical analysis (DMA) thermograms, and mechanical properties of the composite ethylcellulose films were studied. In addition, puncture strength and % elongation of the dry and wet films were also compared from indentation test.

Results. Significant reduction and change in film transparency and morphology was obtained for EC films blended with PVP of higher molecular weight (MW). The composite EC films also showed higher T_g , greater elastic modulus, tensile and puncture strength depending on the concentration and type of additives present.

Conclusions. The interaction between ethylcellulose and the polymeric additives is dependent on the MW and concentration of additives. The composite films offer new opportunities for the use of ethylcellulose as modified release coatings for dosage forms.

KEY WORDS: differential scanning calorimetry; dynamic mechanical analysis; ethylcellulose; mechanical test; polyvinylpyrrolidone.

INTRODUCTION

Ethylcellulose (EC) is a water-insoluble film former with good mechanical and film-forming properties, which enables the formation of flexible and tough coatings (1). In addition, it is available in a wide range of viscosity, soluble in a variety of organic solvents, and miscible with various water-soluble polymers (2,3). These characteristics allow the formulator flexibility in optimizing formulations of EC for coating. EC coating is useful for protection of moisture-sensitive drugs due to its poor permeability to water vapor and poor solubility in water. However, these properties strongly retard drug release and thereby limit the application of pure EC coating in the controlled release of drug. The drug release rate from pellets coated with Aquacoat ECD-30 was poor even when one plasticizer was added (4,5).

Studies undertaken to improve drug permeability through EC coatings included reduction in the thickness of the coating layer (6), formation of pores using organic sol-

vents (7,8), and incorporation of hydrophilic additives (9,10). A number of studies were directed at employing additives to modify the permeability of EC films: hydroxypropyl methylcellulose (11,12), hydroxypropyl cellulose (13), carboxy methylcellulose (14), acrylates (15–17), pectin (18), maltodextrins (19), xylitol (19), and polyethylene glycol (19,20). Among these studies, the influence of hydroxypropyl methylcellulose on the properties of ethylcellulose films has been most extensively investigated. The rate of drug release was often reported to be dependent on the type and proportion of additives added. The molecular weight of the additive and its concentration in the polymeric dispersion were also found to have significant influence on the hardness and elasticity of the film coats.

Hydrophilic additives increase the permeability of hydrophobic films by several mechanisms. For example, polyethylene glycol can dissolve or erode in the release medium and thus create pores in the EC film (21). In contrast, hydroxypropyl cellulose, which dissolves or erodes partially, forms a matrix with EC (22). Some additives modify drug release through EC films by acting as carriers for drugs, such as Span 20 (23) and tetrabutylammonium bromide for salicylic acid.

Polyvinylpyrrolidone (PVP) is a water soluble, physiologically inert synthetic polymer consisting essentially of linear 1-vinyl-2-pyrrolidinone groups, with varying degree of po-

¹ Department of Pharmacy, Faculty of Science, National University of Singapore, Singapore 117543, Singapore.

² To whom correspondence should be addressed. (e-mail: phapaulh@nus.edu.sg)

lymerization that results in polymers of various molecular weights (24–28). PVP has been reported to increase the solubility of active substances by forming water-soluble complexes. Viviprint 540 is a PVP homopolymer that is formed by *in situ* incorporation of insoluble cross-linked poly(PVP) nanoparticles into soluble, film-forming PVP polymer, resulting in formation of molecular-composite PVP (MCPVP) (29). It is therefore of much larger molecular weight than PVP and less soluble in water. It can be used as a binder as well as a top coat in multilayer coating system. The swelling property of cross-linked PVP was used to enhance drug release. In one study, Fan *et al.* (16) developed a system composed of drug and a swelling agent of cross-linked PVP core coated by ethylcellulose/Eudragit L. Eudragit L dissolved in the medium pH above 6, resulting in the formation of pores in the coat. Thus, the medium penetrated through the pores to reach the core, causing the swelling agent to expand and burst the coat to release the drug rapidly. Plasdone S-630 copolyvidonum (PV/VA) is a synthetic water-soluble copolymer consisting of *N*-vinyl-2-pyrrolidone and vinyl acetate in a random 60:40 ratio. It can be used as binder in dry and wet granulation methods. Zingone *et al.* (30) reported that the solubility and dissolution rate of carbamazepine can be enhanced when mixed with PV/VA copolymer possibly due to decrease in crystallinity and increase in wettability of drug.

All the water-soluble polymers discussed above are potential polymeric film modifier for achieving improved drug release. To date, studies on composite EC films containing PVP, MCPVP, and PV/VA for controlled release have not been reported. Incorporation of different additives may cause various changes in molecular interactions within the polymer matrix resulting in altered physicochemical film properties as measured by the moisture permeability, thermal and tensile properties of the matrix (31). It has been reported that changes in the physicochemical properties of films reflected changes in polymer tortuosity and porosity, which can influence drug diffusion. A correlation between the physicochemical properties of cellulose hydrogen phthalate films, as measured by tensile strength and glass transition tempera-

ture (T_g) and drug diffusion, had been demonstrated (32). Films containing dibutyl phthalate exhibited greater tensile strength, higher T_g s, and slower permeation rates than films with added glycerol. It was thought that the increase in T_g and tensile strength of polymer films corresponded to hardening of the films and resulted in depression of drug release rates. Van Bommel *et al.* (33) has also showed that increasing the concentration of acetaminophen in EC films resulted in increase in drug release, while the tensile strength and T_g decreased. Hence, information about the physicochemical and physiochemical properties of composite EC films containing PVP, MCPVP, and PV/VA may be useful for interpretation of release characteristic of drug delivery systems coated with composite EC films.

MATERIALS AND METHODS

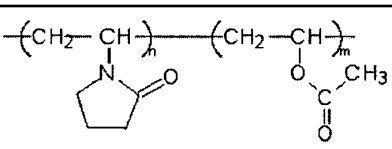
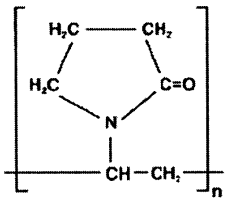
Materials

A commercial EC dispersion (Surelease, Colorcon, West Point, PA, USA) was used as a plasticized aqueous dispersion of EC for film-forming. The following polymeric additives from ISP (Wayne, NJ, USA) were added to ethylcellulose dispersions to form the composite films (Table I): Plasdone K-17 (PVP K17, MW ~8000), Plasdone K-29/32 (PVP K29, MW ~58,000), Plasdone K-60 (PVP K60, MW ~400,000), Plasdone K-90/D (PVP K90, MW ~1,300,000), Plasdone S-630 (PV/VA, MW ~58,000), and Viviprint 540 (MCPVP, MW ~1,500,000–2,000,000).

Preparation of Film-Forming Dispersions

Ten percent to 30% w/w of polymeric additives (based on total solid content of film) were added to an appropriate amount of EC dispersion. The mixture was then diluted with distilled water to 10% w/w of EC and was stirred for 5 h using a magnetic stirrer before it was used to cast films. The control was prepared by diluting an appropriate amount of EC dispersion to give 10% w/w EC, which was then stirred for 1 h.

Table I. Chemical Structures, Typical Molecular Weights, and Viscosity of the Polymeric Additives

Polymeric additives	Chemical structure	K value	Typical molecular weight	Typical viscosity (mPa s)
<i>N</i> -Vinyl-2-pyrrolidone and vinyl acetate copolymer (PV/VA)		25.4–34.2	58,000 ^a	2.5 ^b
Polyvinylpyrrolidone		16–18	8,000 ^a	1.5 ^b
PVP K17		29–32	58,000 ^a	2.5 ^b
PVP K29		50–62	400,000	147 cps
PVP K60		85–95	1,300,000 ^a	55.0 ^b
PVP K90		—	1,500,000–2,000,000 ^d	5,000–20,000 cps ^c
Molecular-composite polyvinylpyrrolidone (MCPVP)				

^a Weight average, determined by light scattering.

^b 5% solution in deionized water. Brookfield LVT viscometer (60 rpm @ 25°C).

^c Brookfield LV, Spindle 4, 12 rpm, @ 25°C.

^d Measured by GPC/MALLS.

Preparation of Films

Films of 200 μm thick were prepared by casting predetermined amounts of film forming dispersions on leveled polytetrafluoroethylene (PTFE)-coated glass plates (casting area = 17 cm \times 17 cm). After 48 h of drying in an oven at 55°C, the films were removed from the glass plates using a sharp knife. Only films that were free from visually evident imperfections, such as cracks or presence of air cavities, were used for subsequent tests.

Evaluation of Film Properties

The free films were cut into strips of specific sizes for determination of various properties. The thickness of each piece of cut film was determined at five locations on the film. Only films with thickness deviation less than 10% of the mean thickness were used for the respective tests. Film samples were aged at room temperature in desiccators containing silica gel for at least 5 days prior to testing.

Differential Scanning Calorimetry

The thermal property of EC and the additives were determined using a differential scanning calorimeter (DSC-50, Shimadzu, Kyoto, Japan), which was coupled with a thermal analyzer (TA-60W, Shimadzu, Kyoto, Japan) to the computer. Films of pure EC, PVP, PV/VA, MCPVP, and polymeric blends were prepared by casting 5% w/w of polymer(s) in solvent mixture of methylene chloride and acetone in the ratio of 5:1 onto a PTFE dish. The film-forming solutions were dried by evaporation at about 30°C for 24 h, and the films were then kept in a desiccator containing silica gel for 5 days before analysis. Accurately weighed, about 5 mg of samples were used for determination of thermal properties of the polymers and polymer blends under nitrogen. The samples were first heated to 200°C at a rate of 20°C/min to erase the previous thermal history and remove any residual moisture. After cooling, a second scan was carried out at a heating rate of 10°C/min to 250°C. The glass transition temperature (T_g) was taken as the temperature corresponding to 50% of the transition (i.e., the midpoint of the discontinuity in heat flow in the second heating cycle).

Dynamic Mechanical Analysis

The thermal mechanical spectra of the films were obtained using dynamic mechanical analyzer (DMA 2980, TA Instruments, New Castle, DE, USA). This technique involved measurement of a sinusoidal strain induced by application of a sinusoidal mechanical force. The response was resolved into part which was in phase with the applied stress (elastic component) and that, which was out of phase with applied stress (viscous component) (34). Changes in these responses were studied as a function of temperature and frequency. For a viscoelastic material, the elastic response (recoverable energy) is represented by the storage modulus E' while the loss modulus E'' is the viscous response (lost energy). The tangent of the loss angle, $\tan \delta$, is equal to the ratio of the energy lost (dissipated as heat) to energy stored per cycle:

$$\tan \delta = \text{loss modulus/storage modulus} = E''/E' \quad (1)$$

This equation applies for response of material changes with temperature at fixed frequency. Thus the profiles of elas-

tic component of the tensile modulus (E') and the mechanical loss ($\tan \delta$) with respect to temperature were obtained. The glass transition of the composite films, T_g , represented by a sharp drop in modulus and a peak for $\tan \delta$, can therefore be determined by DMA.

The instrument consists of a clamp assembly with a plate that is affixed to the drive clamp. The sample with a size of 10 mm \times 5 mm and thickness varying from 0.225 to 0.348 mm is sandwiched between the plate and studs mounted on the fixed clamps. The clamp assembly is surrounded by a furnace that is used to heat and cool the sample. The samples were tested using tension mode and heated from 20°C to 120°C at 3°C/min with a frequency of 1 Hz. The maximum of $\tan \delta$ and/or a sharp drop in modulus was taken as the glass transition temperature. The upper temperature was limited due to the rapidly decreasing mechanical stability of the plasticized samples above their glass transition temperature. All experiments were performed under a dry nitrogen atmosphere.

Characterization of Surface Morphology

Surface morphology of the films was examined using a light microscope (BX 61 Olympus, Tokyo, Japan).

Determination of Film Transparency

The film sample (40 mm \times 25 mm, $n = 3$) was mounted on the cell holder of a spectrophotometer (UV-1201, Shimadzu), and light transmittance at 600 nm through the film was determined. The mean percent transmittance for each film formulation was calculated.

Tensile Testing

The mechanical properties of the films (70 mm \times 10 mm, $n = 6$) were evaluated using a tensile testing instrument (EZ Test-100N, Shimadzu) with a 100 N capacity load cell. The test procedure was based on the ASTM D 882-75d method using flat-faced metal grips with roughened surfaces. The film samples were equilibrated for 1 h at $47 \pm 2\%$ RH and $25 \pm 2^\circ\text{C}$ prior to test. The initial gauge length was 50 mm and the extension speed was 5 mm/min. Four mechanical properties, namely tensile strength, % elongation at break, elastic modulus and work of failure were computed from the load-strain profile as shown below (35):

$$\tau = L_{\text{max}}/A_i \quad (2)$$

$$\varepsilon = \Delta I_b/I_i \quad (3)$$

$$\text{EM} = (dL/dm)/A_i \quad (4)$$

$$\omega = \text{AUC}\delta/A_i \quad (5)$$

where τ is the tensile strength (N/mm²), L_{max} is the maximum load (N), A_i is the initial cross-sectional area of the film sample (mm²), ε is the percent elongation at break (%), ΔI_b is the increase in length at break point (mm), I_i is the initial gauge length (mm), EM is the elastic modulus (N/mm²), dL/dm is the slope of the linear portion of the elastic deformation, ω is the work of failure (J/m²), AUC is the area under the curve (N²/mm⁴), and δ is the cross-head speed (mm/min).

Puncture Test

The puncture test ($n = 3$) was carried out on both dry and wet circular films of diameter 25.2 mm, using a tensile testing instrument (EZ Test-500N, Shimadzu, Kyoto, Japan) with a 500 N capacity load cell. A conical-shaped puncture probe with an angle of 60° and lateral area of 5 cm^2 was attached to the load cell. The film, sandwiched between rubber and PTFE gaskets, was placed over the mouth of a stainless steel cup and secured by an open screw cap. The wet film, immersed in distilled water for 24 h, was blotted dry prior to mounting. The puncture probe was driven downward through the center of the mounted film at a crosshead speed of 5 mm/min, with the load-displacement data recorded from the point of contact of the probe with the film until the film was pierced. Puncture strength and % elongation were derived from the load-displacement profile based on the following equations (36):

$$\gamma = F/A_{cs} \quad (6)$$

$$\delta = [\{ (R^2 + D^2)^{1/2} - R \} / R] 100 \quad (7)$$

where γ is the puncture strength (N/mm^2), F is the load required for puncture, A_{cs} is the cross-sectional area of the film, δ is the % elongation, R is radius of the film exposed across the open screw cap, and D is the displacement of the probe from point of contact to point of puncture.

RESULTS AND DISCUSSION

Thermal and Dynamic Mechanical Analysis

Many methods have been used to study interactions in polymeric blends including, thermoanalytical techniques, microscopy, light scattering, small-angle neutron scattering, inverse gas chromatography, rheology, and spectroscopic techniques (37). Measurement of glass transition temperature (T_g) is one of the most common approaches in studying the behavior of polymer blends (38–40). T_g is the temperature at which the molecular chain of a polymer obtains sufficient energy to surmount the energy barrier for bond rotation (41). Consequently, the polymer changes from a frozen glass-like condition with very limited mobility to a totally mobile system that achieves thermodynamic equilibrium instantaneously. Glass transition is fundamental property of an amorphous material that determines its end-use properties, such as mechanical properties, thermal properties and permeability. Depending on the nature of the interactions between the individual components, polymeric blends may be miscible (single phase), partially miscible, or immiscible (phase separated). In an ideal situation, miscible blends will exhibit a single T_g at an intermediate value, between the T_g s of the individual components. In immiscible blends, the T_g s of the individual components will remain unchanged. When the solubility limit of one of the polymers in a miscible blend is exceeded, phase separation will occur and an additional T_g corresponding to the polymer in the excess will be observed. The final properties of the blend will be determined by the miscibility and the phase behavior of the blend.

In order to determine the miscibility of PVP, PV/VA, and MCPVP with EC, films of individual polymer and polymer blends were prepared from organic solutions. The thermal profiles of pure EC, PVP, PV/VA, and MCPVP films were determined using DSC. In the first heating cycle, the

thermograms were disturbed in the range of $30\text{--}110^\circ\text{C}$ for EC film and $30\text{--}150^\circ\text{C}$ for PVP, PV/VA, and MCPVP samples, possibly due to presence of water or other unknown effects, such as sintering of samples (42). Although the T_g s of EC and MCPVP film samples were prominently detectable from the thermograms of first heating scan, the thermograms of PVP and PV/VA film samples did not show any characteristic slight drop in the heat flow suggestive of T_g . However, T_g s of PVP and PV/VA film samples become visible on second heating scan at 157.1°C and 100.6°C , respectively. The T_g s of EC and MCPVP film determined from the second heating scan were 178.4°C and 178.3°C , respectively.

DSC scans of blends of EC with PVP were also determined and shown in Fig. 1. When PVP was blended with EC, a single endothermic transition in the temperature range $178\text{--}180^\circ\text{C}$, representing the T_g of EC, was exhibited. As the content of PVP increased, the endothermic curve of EC became broader and less prominent. However, the T_g remained constant for EC-PVP blends up to a ratio of 40:60. An additional endothermic transition at around 150°C , representing the T_g of PVP, was observed for EC-PVP (40:60) film. At PVP concentration of 70% and above, the EC endothermic transition disappeared and only the PVP glass transition endotherm was exhibited. The presence of a single concentration dependent T_g lying between the T_g s of the individual components was used as a criterion for establishing polymer-polymer miscibility. In contrast, the presence of two T_g s corresponding to the T_g s of the individual components was an indication of immiscible blends. The results obtained deviated slightly from the ideal. Because addition of 10–50% PVP to EC resulted in a single T_g peak that was close to the T_g of EC, PVP could partially be miscible with EC up to a concentration of 50%. Immiscibility was shown in the EC-PVP (4:6) blend while EC became partially dissolved in PVP when the concentration of PVP was increased to 70% or more.

Generally, the DSC thermograms of EC-MCPVP blends shown in Fig. 2 exhibited a single glass transition endotherm for all the polymer blends. However, as the glass transition endotherms of EC and MCPVP occurred in the similar temperature region of $\sim 178\text{--}180^\circ\text{C}$, it is hard to distinguish if the single endothermic transition in EC-MCPVP blends was due

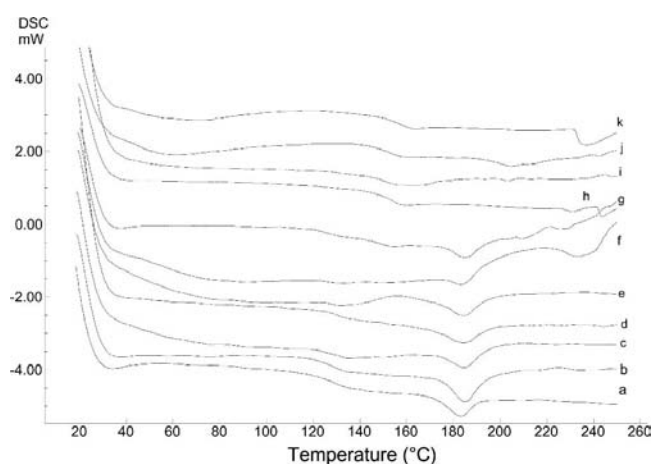


Fig. 1. DSC thermograms of (a) EC, (b) EC-PVP K29 (9:1), (c) EC-PVP K29 (8:2), (d) EC-PVP K29 (7:3), (e) EC-PVP K29 (6:4), (f) EC-PVP K29 (5:5), (g) EC-PVP K29 (4:6), (h) EC-PVP K29 (3:7), (i) EC-PVP K29 (2:8), (j) EC-PVP K29 (1:9), (k) PVP K29.

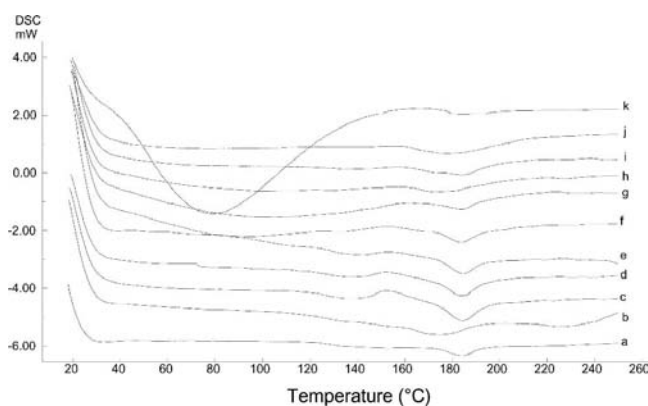


Fig. 2. DSC thermograms of (a) EC, (b) EC-MCPVP (9:1), (c) EC-MCPVP (8:2), (d) EC-MCPVP (7:3), (e) EC-MCPVP (6:4), (f) EC-MCPVP (5:5), (g) EC-MCPVP (4:6), (h) EC-MCPVP (3:7), (i) EC-MCPVP (2:8), (j) EC-MCPVP (1:9), (k) MCPVP.

to the glass transition endotherm of EC or MCPVP or fusion of both polymers. Hence, the DSC results were not conclusive if MCPVP was miscible with EC. It was also observed that with the addition of EC, the broad endotherm of MCPVP in the 30–120°C region disappeared. The broad endotherm of MCPVP may be attributed to presence of water absorbed from environment as MCPVP exhibited hygroscopic nature. Addition of EC at concentration as low as 10% seem to be able to effectively reduce the amount of water absorbed by MCPVP.

The DSC thermograms of EC-PV/VA blends were similar to that of EC-PVP blends (Fig. 3). A single endothermic transition occurring in the region of 170–180°C was observed for EC-PV/VA blends for ratios of 100:0 to 50:50. The endothermic peak of EC gradually diminished as the PV/VA concentration increased to 80%. EC-PV/VA blends in the ratio of 10:90 and 20:80 also presented a single endothermic transition at the 98–100°C region, representing the T_g of PV/VA. On the other hand, two endothermic transitions in the regions of 175–178°C and 98–99°C were obtained for EC-PV/VA blends with the ratios of 40:60 and 30:70. This indicated that PV/VA might be partially miscible with EC for concentration of up to 50%. Compared to PVP, PV/VA showed lesser in-

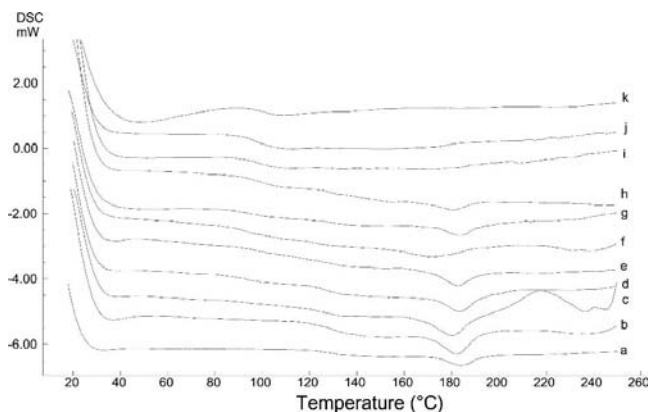


Fig. 3. DSC thermograms of (a) EC, (b) EC-PV/VA (9:1), (c) EC-PV/VA (8:2), (d) EC-PV/VA (7:3), (e) EC-PV/VA (6:4), (f) EC-PV/VA (5:5), (g) EC-PV/VA (4:6), (h) EC-PV/VA (3:7), (i) EC-PV/VA (2:8), (j) EC-PV/VA (1:9), (k) PV/VA.

teraction with EC as the polymer blend showed immiscibility at a lower ratio of 30:70.

Based on the above results, 10–30% w/w PVP, PV/VA, and MCPVP were then added to aqueous EC dispersion, containing plasticizer and stabilizers, to form composite EC films. Further attempt were made to determine any interactions between the polymeric additives and EC dispersion. However, the DSC thermogram of EC film sample prepared from Surelease did not show any T_g value due to the presence of additives in Surelease formulation. In order to study the thermal and mechanical profile of composite EC films, DMA was used. DMA has been reported to be more sensitive to macroscopic as well as molecular relaxation processes compared to other thermal analysis techniques that depend solely on temperature probe (41). It is widely used to determine T_g and miscibility between polymers (34,43–44). Generally, a dynamic thermal analysis profile may show three forms of transition relaxation. The α transition relaxation, which occurs at the highest temperature, is characterized by a large decrease in E' and a maximum in both the E'' and $\tan \delta$ curves near the inflection point of the E' curve. The α transition occurs in the amorphous regions of the polymer with the initiation of cooperative micro-Brownian motion of the molecular chains (45). Hence, α transition relaxation corresponds to the T_g of the polymer. β transition, which occurs at the second highest temperature, is thought to arise due to motion of side groups or smaller unit backbone chains. The γ transition is another transition which occurs below the β transition temperature. In this region, the main chain segments are frozen in and side group motion is made possible by defects in packing in the glassy and crystalline states. It is related to end group rotation, crystalline defects, backbone-chain motions of short segments or group, and phase separation of impurities or diluents (45–48).

Figure 4 showed the typical DMA thermograms of the EC and composite EC films. EC films formed from Surelease produced only a single peak in $\tan \delta$ curve at 77.5°C (Fig. 4A). This peak was taken to be the α transition or T_g of plasticized EC film. This T_g is much lower than that of pure EC film determined by DSC due to the plasticizing effect of medium chain triglycerides present in Surelease. Composite EC films with 10–30% additives, except for PVP K90, also produced a single peak in $\tan \delta$ curve, however at higher temperature (Table II). Composite EC-PVP K90 film showed a smaller peak at 33–54°C. As pure PVP or PV/VA films are too brittle for DMA test, it is not certain whether this smaller peak which appeared in DMA profile of composite EC-PVP K90 film was due to the α transition of PVP polymer or β transition of ethylcellulose films. However, the DSC profile of pure PVP film samples showed that its T_g is 157°C. Presence of any additional peak due to the immiscibility of PVP component with EC should therefore appear between the T_g s of plasticized EC film (77°C) and that of PVP (157°C). Hence, it is unlikely that the small additional peak in DMA profile of composite EC-PVP K90 film is due to T_g of PVP K90. Because all the composite EC films showed a single T_g peak in DMA profile, it may be concluded that PVP, PV/VA, and MCPVP were miscible with EC formed from Surelease at concentration of 30% w/w or below.

Generally, addition of PVP and MCPVP caused a 5–22°C increase in T_g of EC films. The increase in T_g of composite EC films seems to be dependent on the proportion

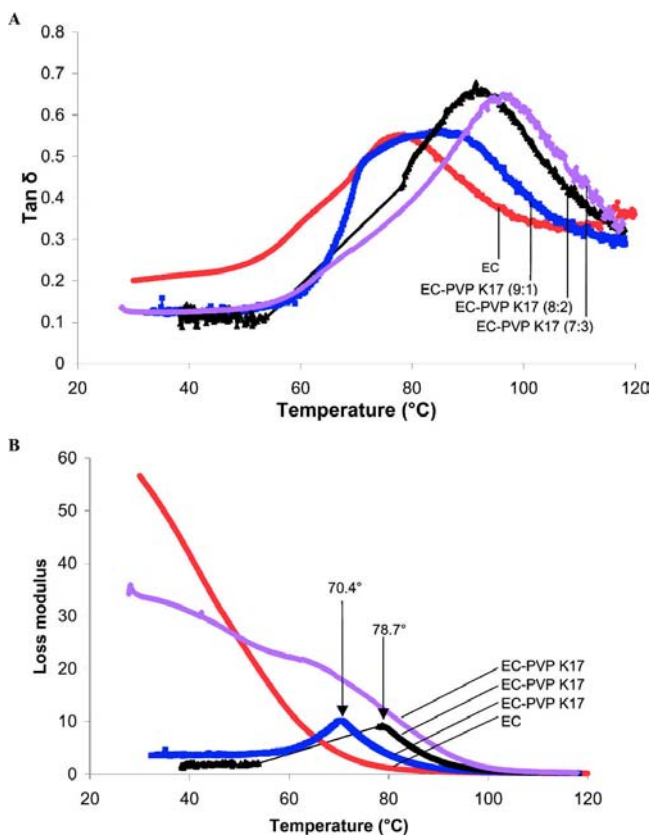


Fig. 4. DMA thermograms: (A) tan δ , (B) loss modulus profiles of EC and EC-PVP K17 films.

of additives present except for PVP K29. A peculiar feature was noted in the DMA thermograms of EC-PVP K17 (9:1) and (8:2) films shown in Fig. 4. Unlike the other film samples, unique sharp peaks were observed for loss modulus of EC-PVP K17 (9:1) and (8:2) films. The peaks occurred at much lower temperatures of 70.4 and 78.7°C than those of tan δ . On the other hand, EC-PVP K17 (7:3) did not show similar peak in its loss modulus profile (Fig. 4B). Both changes in loss modulus and tan δ could indicate occurrence of transition of polymer blend from glass to rubbery state. It may be possible that the lower temperature peaks in loss modulus of EC-PVP K17 (9:1) and (8:2) films indicate possible lower T_g values than that suggested by their tan δ profiles.

When the T_g of the polymer blend is dependent on their concentrations, the Gordon Taylor equation may be applicable for prediction of T_g of polymer blends (49). This equation is based on the additivity of free volumes of the individual components characteristic of ideal mixing (50). It can be expressed as

$$T_{g12} = (w_1 T_{g1} + K w_2 T_{g2}) / (w_1 + K w_2) \quad (8)$$

where T_{g12} is the glass transition temperature of the polymer blend. w_1 , w_2 , T_{g1} , and T_{g2} are the weight fractions and glass transition temperatures of the polymers. The constant, K , is a measure of interaction between the components and can be estimated using the following equation (51),

$$K \sim \rho_1 T_{g1} / \rho_2 T_{g2} \quad (9)$$

where ρ_1 and ρ_2 refer to the true densities of the components. Any difference between the actual T_g and estimated

value would suggest deviation from ideal behavior. Deviation from ideal behavior was often attributed to differences in strength of intermolecular interaction between the individual components and those of the blend. The T_g will be higher than expected if the two polymers bind more strongly to each other than to themselves. This is because stronger binding lowers chain mobility. In contrast, if the polymers bind less strongly with each other than with themselves, the T_g s of the blends are usually lower than expected. The expected T_g values of composite EC blend was calculated and shown in Table II. All the measured T_g values of composite EC films were higher than the expected values, suggesting that EC might interact strongly with the additives.

Among the additives, PV/VA resulted in the smallest increase in T_g of EC films, followed by MCPVP and PVP. In order for the polymers to form compatible blends favorable intermolecular interactions must occur between the different polymer chains (52). These interactions should result in a negative free energy of mixing which can be expressed as

$$\Delta G_M = \Delta H_M - T \Delta S_M \quad (10)$$

where ΔG_M is the free energy of mixing, ΔH_M is the enthalpy of mixing, T is the absolute temperature, and ΔS_M is the entropy of mixing. As the entropy of mixing in polymeric blends is small, the enthalpy of mixing is the primary factor determining whether the components are miscible. A negative enthalpy of mixing can be produced by specific interactions between the constituent polymers, such as hydrogen bonding. Taylor and Zografis (53) had reported hydrogen bond interactions can occur in mixture of amorphous oligosaccharides and PVP between the sugar hydroxyl groups and the proton-accepting carbonyl moiety in the pyrrolidone rings of PVP polymer. Because EC is a partially substituted polysaccharide and given the presence of unsubstituted hydroxyl groups on the cellulose chains, it seems likely that EC may interact with PVP in a similar manner (54).

In certain case, T_g is also a useful parameter for determining the efficiency of plasticizers. Dechesne *et al.* (55) reported that addition of plasticizers to acrylic resin copolymers lowered T_g . The magnitude of change was found to be dependent on the quantity and type of plasticizer used. In this current study, the increase in T_g values by the addition of PVP (except PVP K17), PPVP and PV/VA showed that these additives had no typical plasticizing effect on EC films. In contrast, when present in small amount (10–20%), PVP K17 seemed to result in slight depression in T_g of the composite EC films. This indicated that PVP K17 might be capable of acting as a plasticizer when added in small amount to EC.

Film Morphology

Figure 5 shows the light microscope images of EC and composite EC films (40× magnification). The control EC films appeared smooth and relatively transparent with transmittance of 69.3%. A 25% drop in transmittance of EC film was observed with the addition of PVP K17 (Fig. 6). The reduction in transmittance was independent of the concentration of PVP K17 present. Addition of PVP K29 resulted in 20–51% reduction in film transparency. Unlike PVP K17, greater reduction in transmittance was obtained with higher concentrations of PVP K29. PVP K60 and K90 reduced the film transparency to a much greater extent. Addition of 10%

Table II. Glass Transition Temperature (T_g), Transparency, and Mechanical Properties of EC and Composite EC Films (Mean \pm SD, $n = 6$, Unless Otherwise Indicated)

Films	T_g^a	Estimated T_g	Tensile strength (N/mm ²)	% elongation at break	Elastic modulus (N/mm ²)	Work of failure (KJ/m ²)	Tensile strength/elastic modulus $\times 10^{-2}$
EC	77.5	—	3.17 \pm 0.1	8.34 \pm 0.8	123 \pm 10	11,000 \pm 1100	2.58
EC-PV/VA (9:1)	78.2	79.1	3.59 \pm 0.1 ^c	6.30 \pm 0.6 ^c	179 \pm 7 ^c	8950 \pm 1100	2.09 ^c
EC-PV/VA (8:2)	82.9	80.7	3.86 \pm 0.2 ^c	7.32 \pm 0.5	208 \pm 7 ^c	11,700 \pm 1400	1.86 ^c
EC-PV/VA (7:3)	92.5	82.5	2.93 \pm 0.1	9.53 \pm 0.9	155 \pm 9 ^c	11,800 \pm 1100	1.81 ^c
EC-PVP K17 (9:1)	84.4/70.4 ^b	81.1	2.56 \pm 0.1 ^c	18.70 \pm 5.5	75 \pm 4 ^c	20,300 \pm 6800	3.42
EC-PVP K17 (8:2)	91.5/78.7 ^b	85.2	1.77 \pm 0.1 ^c	15.50 \pm 1.5 ^c	85 \pm 9 ^c	12,000 \pm 1500	2.11
EC-PVP K17 (7:3)	96.3	89.9	3.10 \pm 0.5	4.54 \pm 0.9 ^c	171 \pm 27	5380 \pm 1900 ^c	1.81
EC-PVP K29 (9:1)	99.7	81.1	3.83 \pm 0.1 ^c	6.70 \pm 1.4	198 \pm 7 ^c	10,300 \pm 2700	2.00 ^c
EC-PVP K29 (8:2)	95.7	85.2	3.29 \pm 0.1	13.80 \pm 1.6 ^c	155 \pm 8 ^c	20,300 \pm 2600 ^c	1.85 ^c
EC-PVP K29 (7:3)	98.7	89.9	3.87 \pm 0.1 ^c	9.44 \pm 0.4	199 \pm 1 ^c	13,700 \pm 760 ^c	1.94 ^c
EC-PVP K60 (9:1)	102.0	81.1	2.22 \pm 0.2 ^c	5.04 \pm 1.1 ^c	121 \pm 17	4100 \pm 950 ^c	1.86
EC-PVP K60 (8:2)	99.1	85.2	2.37 \pm 0.1 ^c	8.27 \pm 0.6	123 \pm 5	7920 \pm 570 ^c	1.92
EC-PVP K60 (7:3)	102.2	89.9	2.28 \pm 0.2 ^c	10.40 \pm 2.2	119 \pm 16	9910 \pm 2700	1.93
EC-PVP K90 (9:1)	96.6	81.1	3.22 \pm 0.2	9.70 \pm 1.6	155 \pm 12 ^c	13,200 \pm 2700	1.93 ^c
EC-PVP K90 (8:2)	97.6	85.2	3.95 \pm 0.1 ^c	10.60 \pm 3.0	212 \pm 10 ^c	18,300 \pm 5500	2.11 ^c
EC-PVP K90 (7:3)	99.4	89.9	4.03 \pm 0.1 ^c	4.93 \pm 0.9 ^c	222 \pm 12 ^c	7510 \pm 780 ^c	1.88 ^c
EC-MCPVP (9:1)	82.7	82.1	2.29 \pm 0.2 ^c	5.73 \pm 2.3	111 \pm 6	4530 \pm 3000	2.07 ^c
EC-MCPVP (8:2)	94.6	87.4	3.21 \pm 0.2	5.31 \pm 1.3 ^c	178 \pm 6 ^c	6730 \pm 2200	1.80 ^c
EC-MCPVP (7:3)	98.6	93.3	3.27 \pm 0.6	6.03 \pm 3.9	188 \pm 11 ^c	8690 \pm 6900	1.73 ^c

^a $n = 1$, values obtained from maxima of $\tan \delta$ unless otherwise stated.

^b Values obtained from loss modulus.

^c Significant at $p < 0.05$ compared to EC film.

PVP K90 reduced the film transparency by 58% while almost opaque films, with a transmittance of 2.14%, were obtained when 30% w/w of the additive was used. Similarly, MCPVP drastically reduced the transparency of EC films. As the above additives vary in molecular weights, the results suggested that molecular size of PVP greatly affected the clarity of composite EC films.

In composite polymer films, the major component generally forms the matrix while the minor component dispersed in the form of spherical domains. For example, blends of EC and hydroxypropylmethylcellulose exhibit single layer morphologies with inclusions of the minor phase dispersed in the major polymer (56). Immiscibility between two polymers could be manifested in separation of film layers. In one study, composite EC-cellulose acetate phthalate (1:1) films were found to separate into two distinct layers, with EC rich layer on top and cellulose acetate phthalate rich layer below (57). Figure 5 showed the light microscopy image of EC film as a continuous, homogenous layer with few holes. With the addition of low-molecular-weight PVP (K17 and K29), small circular crevices randomly dispersed throughout the film layer were observed. Increasing the concentration of PVP K17 or K29 resulted in greater number of crevices as well as slight increase in size of the crevices. Hence, it was thought that the crevices could be attributed to the presence of PVP K17 or K29 randomly dispersed through the EC matrix. Similar observation was seen in the presence of low amount (10%) of higher molecular weight PVP (K60 and K90). However, with greater amount of PVP K60 (30%) or PVP K90 (20%), a separate irregular network-like layer was prominently exhibited above a less obvious layer. At even higher concentration of PVP K60 or K90, the composite EC films appeared as dense layer with several small holes. This suggested that at

concentration of 20% or more, higher molecular weight PVP may have aggregated together to form a separate layer during film drying. Similar pattern of irregular network-like layer was seen for composite EC-MCPVP films containing MCPVP concentration as low as 10%. At higher concentration of MCPVP, the composite EC films became denser as with EC-PVP K90 films.

When taken together with the film transparency results, higher concentrations of large-molecular-weight polymers, PVP and MCPVP, may not be fully miscible with EC. At high concentration, the large-molecular-weight PVP and MCPVP have a tendency to aggregate during the drying process to form a separate phase, resulting in separate coating on the top surface of the film in contrast to a homogenous layer with the additives of lower concentration, interspersed in the EC matrix. The higher molecular weight PVP was observed to have a greater observable effect probably because their larger molecular size and hence greater tendency to separate forming PVP-rich regions during drying even at low concentration. In contrast, addition of 20–30% PV/VA only resulted in comparatively less decrease in film transparency (Fig. 6). Unlike PVP, composite EC-PV/VA (9:1) films were generally smooth. However, as the amount of PV/VA increased, a separate irregular network-like layer was observed, especially at 30%. This suggested that PV/VA at low concentration was miscible with EC, forming homogeneous and smooth films. However, beyond certain concentration, PV/VA may also aggregate together and form a separate layer.

Based on the above observation, a model for interaction between EC and PVP, MCPVP or PV/VA was postulated. The interaction between EC and PVP polymeric additives was found to be dependent on the molecular weight, concentration, and chemical nature of the additives. When added to

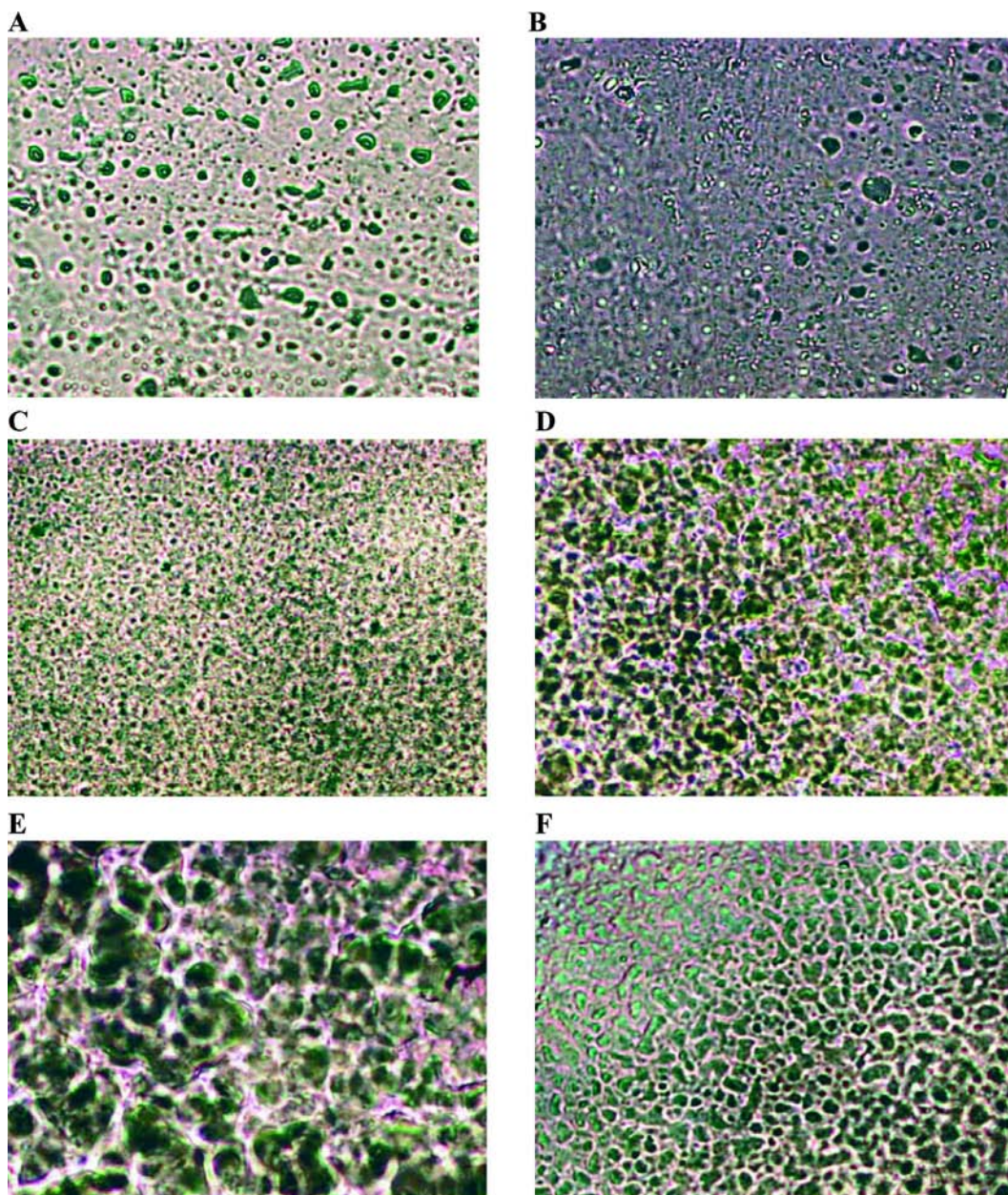


Fig. 5. Light microscope images of EC and composite EC films: (A) EC, (B) EC-PVP K17 (9:1), (C) EC-PVP K29 (9:1), (D) EC-PVP K90 (9:1), (E) EC-MCPVP (9:1), (F) EC-PV/VA (7:3).

EC, low-molecular-weight PVP would be randomly distributed through the EC matrix as shown in Fig. 7B. As the concentration of polymeric additives increased, low-molecular-weight PVP remained as a disperse phase portrayed as greater number of crevices in the continuous EC phase (Fig. 7C). The crevices may increase in size probably due to fusion with neighboring crevices. On the other hand, the interaction between EC and higher molecular weight PVP as represented by PVP K60, K90, and MCPVP were more drastic. At low concentration, higher molecular weight PVP existed as a disperse phase in EC matrix (Fig. 7C). However, as the concentration increased, the higher molecular weight additives tend to aggregate together forming a separate continuous phase (Fig. 7D). Formation of separate continuous layers became more prominent with increasing concentration

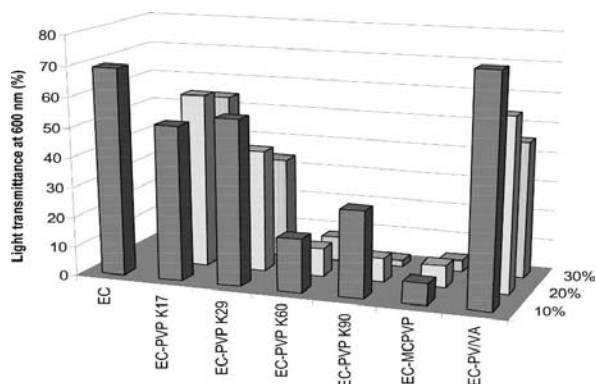


Fig. 6. Effects of types and concentrations of polymeric additives on the film transparency of EC films.

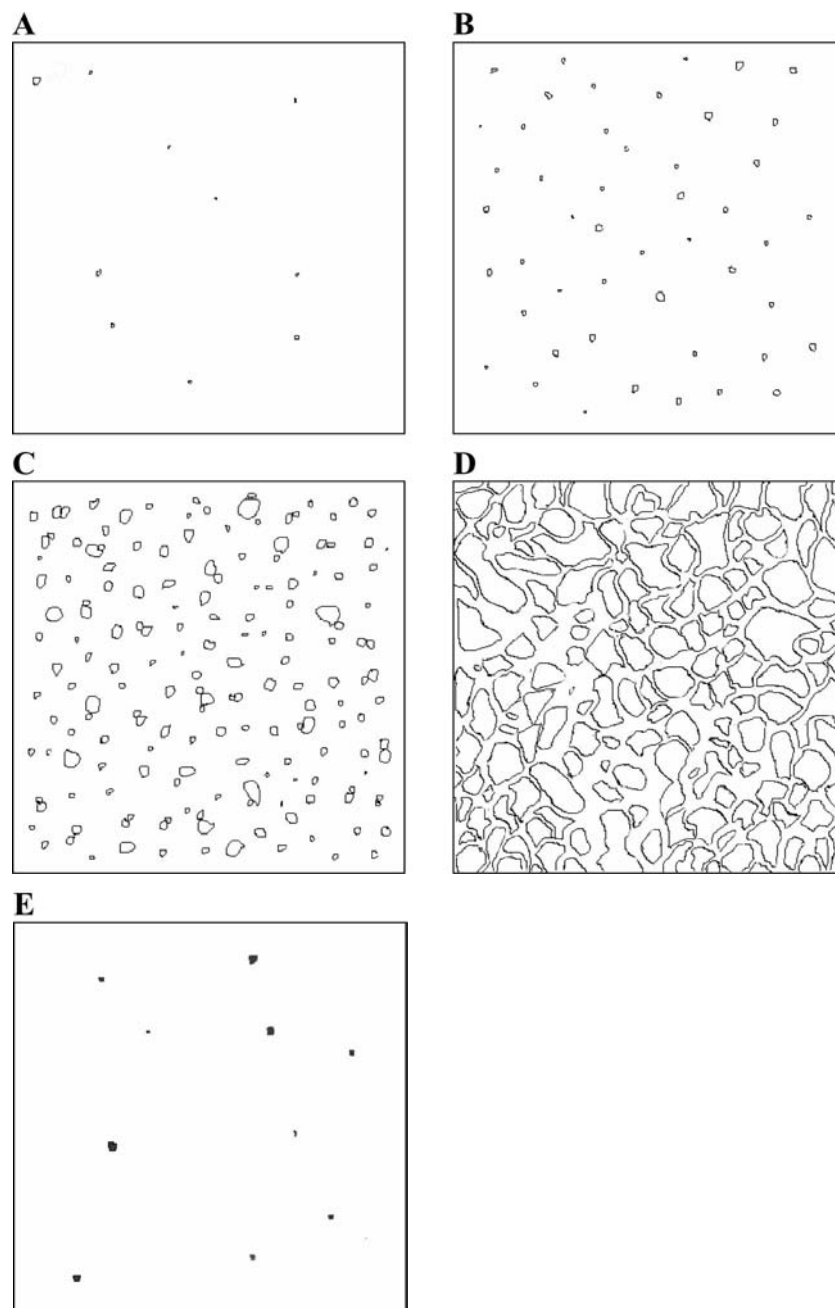


Fig. 7. Model of interaction between PVP, MCPVP, or PV/VA with EC: (A) continuous phase of EC film without polymeric additives, (B) minor component existing as random spheres/crevices in the continuous phase of EC, (C) minor component existing as random spheres/crevices of larger size in the continuous phase of EC, (D) minor component forming a separate continuous phase, (E) overcoat of one continuous phase over another.

portrayed as huge patches or coat above the main film layer (Fig. 7E). Increased in molecular weight of additives may accelerate the formation of separate layers. When the molecular weight is high enough, a separate continuous phase may be formed even at low concentration of 10%, as in the case of MCPVP.

Tensile Test

The stability of film coat on a dosage form to withstand handling and prolonged storage is of major concern to the

formulator. The desired mechanical characteristics of a polymer film are hardness, toughness, and extendability (58–59). Many studies have shown that the occurrence of adhesion and cohesion related film coating defects are mainly due to the building up of internal stresses within the film coat (60–61). These internal stresses have been shown to be due to

1. shrinkage of film after its solidification point as further solvent evaporates from the system (62);
2. the differences between the thermal expansion coefficient of the film coat and the tablet substrate, and the dif-

ference between the glass transition temperature of the film coat and the actual temperature of the film at any time (63); and

3. any volumetric changes in the tablet core occurring during coating and subsequent storage (64–65).

When the total internal stress exceeded the tensile strength of the film, defects such as cracking, edge splitting, and peeling can occur. Hence polymeric films with high tensile strength may be able to withstand the internal stresses better and less likely to result in film defects. Commercial EC pseudolatexes produced rigid and brittle films, thus impairing the stress resistance of the coating (36). This property is undesirable in application where coating of high flexibility and toughness is required (e.g., in tablets compressed from coated beads or cores with deep logos and break lines). Therefore it is important to investigate if addition of polymeric additives has any effect on the mechanical property of EC film.

Table II shows the mechanical properties of EC and composite EC films. EC films formed from aqueous dispersion were found to be weaker and more brittle than those prepared using organic solvents, probably due to different mechanisms of film formation (66). Generally, the addition of PVP increased the tensile strength of composite EC films slightly, except for composite EC films containing PVP K17 or K60. Tensile strength of composite EC films increased to small amount with increasing content of PVP K90. In contrast, the increase in tensile strength of EC-PVP K29 films did not appear to be dependent on the concentration of PVP K29. Composite EC films containing PVP K17 and K60 showed significantly lower tensile strength compared to EC films. In fact, the tensile strength of composite EC film containing 10%w/w PVP K17 was almost 50% lower than that of EC film. Addition of PVP K17 also affected that the % elongation at break of EC film significantly. Presence of PVP K17 up to 20% made EC film more flexible with a higher % elongation at break. However, with 30% PVP K17, the EC film become much less flexible as the % elongation at break value dropped to 4.54. Similar trend was also observed for the hardness of composite EC-PVP K17 films, with significant drop in elastic modulus when 10–20% PVP K17 was added to EC films. These observations suggested that PVP K17 at low concentration ($\leq 20\%$) has a plasticizing effect on EC film.

The addition of PVPs of higher molecular weight than PVP K17 did not affect the % elongation at break of EC films except for films containing 20% PVP K29 and 30% PVP K90. EC-PVP K90 (7:3) film was comparatively more brittle than EC films, as shown by its significantly lower % elongation value. Unlike EC-PVP K17 films, all the rest of EC-PVP films showed significantly higher elastic modulus values than the EC film. Addition of 10–20% PVP K90 caused the elastic modulus of EC films to increase by 26–72%. However, further increase in PVP K90 content to 30% did not result in further significant rise in elastic modulus.

The increase in elastic modulus and tensile strength indicated that the addition of PVP increased the hardness of EC film. EC film is rigid in nature due to the bulky glucose subunits of the polymer, as well as the alkyl substituents serve as sites for potential inter- and intramolecular interactions (36,38). PVP is also a large molecule consisting of polar imide group, four non-polar methylene groups and a methane group. Hence, these molecules can interact through dipole-

dipole attraction and forms hard and clear films (67). Moreover, the ether and hydroxyl groups of EC could also interact with the imide and carbonyl group of PVP via hydrogen bonding. These interactions may also enhanced the strength of the composite films.

Interestingly, when MCPVP was added to EC, the tensile strength decreased or remained unchanged while the % elongation at break dropped to 5.31. Addition of 10% MCPVP did not result in significant change in elastic modulus. However, the elastic modulus increased significantly when the amount of MCPVP was increased to 20% or higher. The increase in elastic modulus of EC-MCPVP was comparatively smaller than that of EC-PVP K90 films. Although MCPVP has higher molecular weight than PVP K90, it has fewer sites available for intermolecular interaction due to the cross-linking. This probably explained the above observations. The EC-MCPVP films, at all concentration of MCPVP, were also less flexible and more brittle than the EC films. This suggested that some of MCPVP molecules were interposed among the EC-rich region. Being large in size, the interposed MCPVP would weaken the intermolecular bonding between the EC chains, causing the film to be more brittle. However, larger amounts of MCPVP enabled the formation of MCPVP rich region above the EC layer, thereby forming a dense film. The intermolecular bonding between MCPVP molecules was thought to be greater than those between EC and MCPVP. Hence, resulting in exhibition of slightly harder and tougher properties.

Addition of PV/VA increased the tensile strength and elastic modulus of the film. Beyond 20% of PV/VA, the films showed lower tensile strength, elastic modulus and work of failure. PV/VA which has similar molecular weight as PVP K29, is less hygroscopic than PVP, due to its vinyl acetate copolymer. In addition to the polar imide group and carbonyl group from its *N*-vinyl-2-pyrrolidone component, PV/VA also has a carbonyl group from its vinyl acetate copolymer, which can participate in intermolecular hydrogen bonding. Therefore, PV/VA would likely interact to a greater extent with EC, forming stronger films than PVP K29. However, this was not reflected in the tensile strength and elastic modulus values of EC-PV/VA films, which were comparable to EC-PVP K29 films.

An important parameter for evaluating the mechanical properties of film coatings applied to tablets is the incidence of cracking or edge splitting (60,68). The occurrence of film coating defects has been associated with the magnitude of internal stress in the film. Rowe (64) suggested that the overall internal stress, P , in a film coat can be represented as follows:

$$P = EM/3(1 - \nu)[(\phi_s - \phi_r)/(1 - \phi_r) + \Delta\alpha_{\text{cubic}}\Delta T] \quad (11)$$

where EM is the Young's modulus of the film, ν its Poisson's ratio, ϕ_s the volume fraction of the solvent at the solidification point of the coating formulation, ϕ_r the volume fraction of solvent remaining in the dry film at ambient conditions, $\Delta\alpha_{\text{cubic}}$ the difference between the thermal cubical expansion coefficients of the coating and the tablet core, and ΔT the difference between the glass transition temperature of the coating and the ambient temperature. Cracking will occur if P is greater than or equal to the tensile strength, τ , of the film (63).

$$P \geq \tau \quad (12)$$

Combining and rearranging both equations gives

$$\tau/EM \leq 1/3(1 - \nu)[(\phi_s - \phi_r)/(1 - \phi_r) + \Delta\alpha_{\text{cubic}}\Delta T] \quad (13)$$

Hence, τ/EM may be used to predict the incidence of edge splitting of a film coat (60). The larger its value the higher the stress crack resistance of a film. In this study, the EC films without additives showed the highest ratio of 0.0258. Addition of PVP, MCPVP, and PV/VA caused a significant drop in the ratio to varying extent. Hence, there was a limit to the concentration of additives that could be added to EC in order not to compromise the stress crack resistance of the final film. The lowest ratio was obtained for EC-MCPVP (7:3) films, suggesting that MCPVP might cause greater impairment to flexibility of EC films particularly at concentration greater than 10%.

Puncture Test

Polymeric coatings may be applied to particles that will be compressed into tablets. Hence, they should have the required resistance to damage caused by compression. Radebaugh *et al.* (69) has reported a new device that can determine the process of puncture on polymeric films directly. It measures the resistance of a film sample, which is mounted on a fixed holder, to deformation with a puncturing probe attached to a force transducer. Due to its design, this test also enables the study of wet film samples, which is difficult to test using the tensile test method. The mechanical properties of wetted film under puncture stress is useful for predicting how polymeric films that would behave during dissolution studies or under *in vivo* conditions (70).

Two parameters, puncture strength and % elongation, were derived from the load-displacement profiles (Table III). When the EC films were soaked in water for 24 h at 37°C, the puncture strength only decreased slightly from 0.378 to 0.332, while a big increase in the % elongation was observed from

0.192 to 0.821. This showed that water has a plasticizing effect on EC film, resulting in films with greater flexibility upon wetting. Addition of PVP, except for PVP K17 and 10% PVP K90, generally increase the puncture strength of dry EC films. The increase in puncture strength appeared to be related to the amount of PVP added, with greater increase observed with a higher concentration of PVP. The influence of concentration of PVP on the % elongation of dry EC films was less obvious as the values fluctuated. Nevertheless, addition of 30% PVP resulted in the highest % elongation for dry EC films. On the contrary, opposite trend was observed for wet EC-PVP films. Except for PVP K17, the highest puncture strength and % elongation was obtained for wet composite EC-PVP containing the lowest concentration of PVP and increasing amount of PVP generally decreased the puncture strength and % elongation.

The results from indentation test of dry EC films were similar to that determined from tensile test. Both tests showed that the composite films became harder with the presence of PVP. However, EC films containing PVP K17 showed a slight drop in puncture strength and increase in % elongation. These observations suggested that PVP K17 might have some plasticizing effect on EC films as discussed earlier. The mechanical properties of wet composite EC-PVP films provide additional insight into the structural arrangement between EC and PVP. When soaked in water for 24 h, the water-soluble PVP interspersed within the EC matrix would dissolve forming crevices filled with water. This largely weakened the EC matrix and resulted in decrease in puncture strength and % elongation. PVP K90 asserted a greater weakening effect on EC matrix than PVP K29, as shown by the lower puncture strength and % elongation of wet EC-PVP K90 films.

The above phenomenon was also observed for both dry and wet composite EC-PPVP films. However, increasing PV/

Table III. Mechanical Properties of Dry and Wet EC and Composite EC Films (Mean \pm SD, n = 4)

Films	Puncture strength (N/mm ²)		% elongation	
	Dry	Wet	Dry	Wet
EC	0.378 \pm 0.00	0.332 \pm 0.03	0.192 \pm 0.06	0.821 \pm 0.28
EC-PV/VA (9:1)	0.182 \pm 0.01	0.192 \pm 0.03	0.079 \pm 0.02	0.481 \pm 0.20
EC-PV/VA (8:2)	0.458 \pm 0.02	0.286 \pm 0.03	0.056 \pm 0.00	2.170 \pm 0.58 ^a
EC-PV/VA (7:3)	0.839 \pm 0.09	0.432 \pm 0.04	0.258 \pm 0.07	1.380 \pm 0.45 ^a
EC-PVP K17 (9:1)	0.265 \pm 0.00 ^a	0.135 \pm 0.04	0.159 \pm 0.03	0.136 \pm 0.01 ^a
EC-PVP K17 (8:2)	0.317 \pm 0.01	0.184 \pm 0.03	0.297 \pm 0.06	0.262 \pm 0.02 ^a
EC-PVP K17 (7:3)	0.376 \pm 0.02 ^a	0.169 \pm 0.02	0.198 \pm 0.03	0.143 \pm 0.04 ^a
EC-PVP K29 (9:1)	0.531 \pm 0.02 ^a	0.322 \pm 0.03	0.184 \pm 0.01 ^a	1.470 \pm 0.08
EC-PVP K29 (8:2)	0.410 \pm 0.02 ^a	0.152 \pm 0.02	0.122 \pm 0.02	0.189 \pm 0.02 ^a
EC-PVP K29 (7:3)	0.983 \pm 0.20	0.231 \pm 0.06	0.280 \pm 0.15	0.570 \pm 0.61
EC-PVP K60 (9:1)	0.396 \pm 0.05	0.145 \pm 0.02	0.162 \pm 0.05 ^a	0.272 \pm 0.15
EC-PVP K60 (8:2)	0.558 \pm 0.06	0.130 \pm 0.01	0.272 \pm 0.03 ^a	0.195 \pm 0.02 ^a
EC-PVP K60 (7:3)	0.607 \pm 0.06	0.109 \pm 0.00	0.280 \pm 0.04 ^a	0.180 \pm 0.05 ^a
EC-PVP K90 (9:1)	0.298 \pm 0.04 ^a	0.164 \pm 0.01	0.159 \pm 0.01 ^a	0.230 \pm 0.02
EC-PVP K90 (8:2)	0.434 \pm 0.02 ^a	0.156 \pm 0.04	0.136 \pm 0.02 ^a	0.203 \pm 0.09 ^a
EC-PVP K90 (7:3)	0.666 \pm 0.11	0.102 \pm 0.02	0.254 \pm 0.03 ^a	0.170 \pm 0.06 ^a
EC-MCPVP (9:1)	0.267 \pm 0.01 ^a	0.201 \pm 0.02	0.144 \pm 0.02 ^a	0.553 \pm 0.21
EC-MCPVP (8:2)	0.470 \pm 0.07 ^a	0.093 \pm 0.01	0.172 \pm 0.01 ^a	0.245 \pm 0.05 ^a
EC-MCPVP (7:3)	0.824 \pm 0.04	0.047 \pm 0.01	0.374 \pm 0.09 ^a	0.809 \pm 0.12 ^a

^a Significant at p < 0.05 compared to EC film.

VA concentration resulted in increasing puncture strength and % elongation for both dry and wet films. Addition of 10% PV/VA reduced the puncture strength and % elongation of the dry and wet films by 50%. However with greater amount of PV/VA, the puncture strength of composite EC-PV/VA films increased to as high as 0.839 N/mm² when dry and 0.432 N/mm² when wet. The % elongation of wetted EC-PV/VA films also increased to almost twice as high suggesting that the wet EC-PV/VA films were more "intact" or compact, allowing the water molecules to be retained in the matrix where they exerted a plasticizing effect.

It was also noted that with 30% of additives, puncture strength of dry composite EC films decrease in the following order: EC-PVP K29 > EC-PV/VA > EC-MCPVP > EC-PVP K90 > EC-PVP K60 > EC-PVP K17. In contrast, the puncture strength of wet composite EC films generally decreased in the following order: EC-PV/VA > EC-PVP K29 > EC-PVP K17 > EC-PVP K60 > EC-PVP K90 > EC-MCPVP. As discussed earlier, MCPVP in high concentration probably formed a separate layer above the EC matrix. When the composite film was soaked in water, MCPVP, which was soluble in water, would dissolve, leaving a thin and weak EC matrix. All composite EC films except for those containing 30% PV/VA, have lower puncture strength than EC films when soaked in water for 24 h.

CONCLUSIONS

Polymers consists of molecular chains that permits buildup of secondary intermolecular forces, such as hydrogen, van der Waals, and dipole-dipole bonds. The magnitude of these interactions is mainly influence by the molecular weight of the polymer, the packing and orientation of the molecular segments, and the flexibility of the polymer chains (71). Hence, it would be useful to have a fundamental understanding of the components of film coating formulations and the interplay between them, which can help in prediction of the end-use properties of film coatings such as permeability, mechanical characteristics, and drug release profile (68).

In this study, it was found that EC films formed from aqueous dispersion were smooth and relatively transparent. Addition of PVP, especially high-molecular-weight PVP, and MCPVP resulted in drastic reduction in film transparency, suggesting that molecular weight of PVP greatly affects the clarity of composite EC films. The interaction between EC and PVP polymeric additives was found to be dependent on the molecular weight, concentration, and chemical nature of the additives. When added to EC, low-molecular-weight PVP would be randomly distributed through the EC matrix as a disperse phase. Increased concentration up to 30% did not alter the phase distribution. In contrast, greater interaction was exhibited between EC and higher molecular weight PVP as represented by PVP K60, K90, and MCPVP. At low concentration, higher molecular weight PVP may exist as a disperse phase in EC matrix. However, as the concentration increased, the higher molecular weight additives tend to aggregate together, forming a separate continuous phase. Formation of separate continuous layers became more prominent with increasing concentration. Increase molecular weight of additives accelerated the progression to formation of separate layers.

At low concentration, PVP increased the hardness of EC

films probably due to intermolecular interaction between EC and PVP. However, addition of large amount of high-molecular-weight PVP or MCPVP would result in polymer phase separation. Incorporation of PVP increased the puncture strength and % elongation of dry films but lowered the puncture strength and % elongation of wet films. On the other hand, PV/VA increased the % elongation of wet films, while the dry films remained brittle. This suggested that wet EC-PV/VA films were more "intact" or compact than EC-PVP films, allowing the water molecule to be retained in the matrix where they exerted their plasticizing effect. The concentration of PVP, MCPVP, or PV/VA used had a significant influence on the flexibility of the resultant films. Addition of PVP, MCPVP, and PV/VA resulted in increase in T_g , tensile strength, and elastic modulus. Relationship between changes in these parameters and water vapor and drug permeabilities will be further investigated and discussed in a subsequent study.

ACKNOWLEDGMENTS

The authors gratefully thank Dr. Pramoda at IMRE for use of the dynamic mechanical analyzer.

REFERENCES

1. G. V. Savage and C. T. Rhodes. The sustained release coating of solid dosage Forms: A historical review. *Drug Dev. Ind. Pharm.* **21**:93-118 (1995).
2. S. C. Porter. Controlled-release film coatings based on ethylcellulose. *Drug Dev. Ind. Pharm.* **15**:1495-1521 (1989).
3. G. S. Rekhii and S. S. Jambhekar. Ethylcellulose—a polymer review. *Drug Dev. Ind. Pharm.* **21**:61-77 (1995).
4. B. C. Lippold, B. K. Sutter, and B. C. Lippold. Parameters controlling drug release from pellets coated with aqueous ethyl cellulose dispersion. *Int. J. Pharm.* **54**:15-25 (1989).
5. W. Gunder, B. H. Lippold, and B. C. Lippold. Release of drugs from ethylcellulose microcapsules (diffusion pellets) with pore formers and pore fusion. *Eur. J. Pharm. Sci.* **3**:203-214 (1995).
6. H. P. Osterwald. Properties of film-formers and their use in aqueous systems. *Pharm. Res.* **2**:14-18 (1985).
7. S. Narisawa, H. Yoshino, Y. Hirakawa, and K. Noda. Porosity-controlled ethylcellulose film coating. I. Formation of porous ethylcellulose film in the casting process and factors affecting film-density. *Chem. Pharm. Bull. (Tokyo)* **41**:329-334 (1993).
8. S. Narisawa, H. Yoshino, Y. Hirakawa, and K. Noda. Porosity-controlled ethylcellulose film coating. II. Spontaneous porous film formation in the spraying process and its solute permeability. *Int. J. Pharm.* **104**:95-106 (1994).
9. M. A. Frohoff-Hulsmann, B. C. Lippold, and J. W. McGinity. Aqueous ethyl cellulose dispersion containing plasticizers of different water solubility and hydroxypropyl methylcellulose as coating material for diffusion pellets II: properties of sprayed films. *Eur. J. Pharm. Biopharm.* **48**:67-75 (1999).
10. M. A. Frohoff-Hulsmann, A. Schmitz, and B. C. Lippold. Aqueous ethyl cellulose dispersions containing plasticizers of different water solubility and hydroxypropyl methylcellulose as coating material for diffusion pellets I. Drug release rates from coated pellets. *Int. J. Pharm.* **177**:69-82 (1999).
11. C. A. Gilligan and A. L. Wan Po. Factors affecting drug release from a pellet system coated with an aqueous dispersion. *Int. J. Pharm.* **73**:51-68 (1991).
12. J. Hjertstam and T. Hjertberg. Swelling of pellets coated with a composite film containing ethylcellulose and hydroxypropyl methylcellulose. *Int. J. Pharm.* **161**:23-28 (1998).
13. K. Umprayn, P. Chitropas, and S. Amarekajorn. Development of terbutaline sulfate sustained-release coated pellets. *Drug Dev. Ind. Pharm.* **25**:477-491 (1999).
14. T. Yamada, H. Onishi, and Y. Machida. Sustained release keto-

- profen microparticles with ethylcellulose and carboxymethylcellulose. *J. Control. Release* **75**:271–282 (2001).
15. C. Sánchez-Lafuente, M. T. Faucci, M. Fernández-Arévalo, J. Álvarez-Fuentes, A. M. Rabasco, and P. Mura. Development of sustained release matrix tablets of didanosine containing methacrylic and ethylcellulose polymers. *Int. J. Pharm.* **234**:213–221 (2002).
 16. T. Y. Fan, S. L. Wei, W. W. Yan, D. B. Chen, and J. Li. An investigation of pulsatile release tablets with ethylcellulose and Eudragit L as film coating materials and cross-linked polyvinylpyrrolidone in the core tablets. *J. Control. Release* **77**:245–251 (2001).
 17. W. Phuapradit, N. H. Shah, A. Railkar, L. Williams, and M. H. Infeld. In vitro characterization of polymeric membrane used for controlled release application. *Drug Dev. Ind. Pharm.* **21**:955–963 (1995).
 18. G. S. Macleod, J. T. Fell, and J. H. Collett. Studies on the physical properties of mixed pectin/ethylcellulose films intended for colonic drug delivery. *Int. J. Pharm.* **157**:53–60 (1997).
 19. B. D. Rohera and N. H. Parikh. Influence of type and level of water-soluble additives on drug release and surface and mechanical properties of Surelease films. *Pharm. Dev. Technol.* **7**:421–432 (2002).
 20. P. Sakellariou, R. C. Rowe, and E. F. T. White. Polymer/polymer interaction in blends of ethylcellulose with both cellulose derivatives and polyethylene glycol 6000. *Int. J. Pharm.* **34**:93–103 (1986).
 21. M. Donbrow and M. Friedman. Enhancement of permeability of ethylcellulose films for drug penetration. *J. Pharm. Pharmacol.* **27**:633–646 (1975).
 22. M. Donbrow and Y. Samuelov. Zero order drug delivery from double-layered porous films: release rate profiles from ethyl cellulose, hydroxypropyl cellulose and polyethylene glycol mixtures. *J. Pharm. Pharmacol.* **32**:463–470 (1980).
 23. T. Lindholm and M. Juslin. Controlled release tablets: Part 3: Ethylcellulose coats containing surfactant and powdered matter. *Pharm. Ind.* **44**:937–941 (1982).
 24. A. Wade and P. J. Weller. Povidone. In A. H. Kibbe (ed.), *Handbook of Pharmaceutical Excipients*, 2nd edition. Pharmaceutical Press, London, 1994, pp. 392–399.
 25. L. Blecher, D. H. Lorenz, H. L. Lowd, A. S. Wood, and D. P. Wyman. Polyvinylpyrrolidone. In R. L. Davidson (ed.), *Handbook of Water-Soluble Gums and Resins*. McGraw-Hill, New York, 1980, Chap. 21, pp. 21–21–22.
 26. B. A. S. F. Fine Chemicals. Kollidone® grades, MEF 129e. BASF Corporation Chemicals Division, Ludwigshafen, Germany, 1986.
 27. C. M. Aldeyeye and E. Barabas. Polyvinylpyrrolidone (Povidone). *Analytic Profiles Drug Substances Excipients* **22**:555–685 (1993).
 28. V. Kumar, T. Yang, and Y. Yang. Interpolymer complexation. Part 1. Preparation and characterization of a polyvinyl acetate phthalate-polyvinylpyrrolidone (PVAP-PVP) complex. *Int. J. Pharm.* **188**:221–232 (1999).
 29. D. K. Hood, L. Senak, S. L. Kopolow, M. A. Tallon, Y. T. Kwak, D. Patel, and J. Mckittrick. Structural insights into a novel molecular-scale composite of soluble poly(vinyl pyrrolidone) supporting uniformly dispersed nanoscale poly(vinyl pyrrolidone) particles. *J. Appl. Polym. Sci.* **89**:734–741 (2003).
 30. G. Zingone and F. Rubessa. Release of carbamazepine from solid dispersions with polyvinylpyrrolidone/vinyl acetate copolymer (PVP/VA). *STP Pharma Sci.* **4**:122–127 (1994).
 31. M. Dittgen, M. Durrani, and K. Lehmann. Acrylic polymers—a review of pharmaceutical applications. *STP Pharma. Sci.* **7**:403–437 (1997).
 32. S. Benita, P. Dor, M. Aronhime, and G. Marom. Permeability and mechanical properties of a new polymer: cellulose hydrogen phthalate. *Int. J. Pharm.* **33**:71–80 (1986).
 33. E. M. G. VanBommel, J. G. Fokkens, and D. J. A. Crommelin. Effects of additives on the physicochemical properties of sprayed ethylcellulose films. *Acta Pharm. Technol.* **35**:232–237 (1989).
 34. S. V. Lafferty, J. M. Newton, and F. Podczek. Dynamic mechanical analysis studies of polymer films prepared from aqueous dispersion. *Int. J. Pharm.* **235**:107–111 (2002).
 35. P. W. S. Heng, L. W. Chan, and K. T. Ong. Influence of storage conditions and type of plasticizers on ethylcellulose and acrylate films formed from aqueous dispersions. *J. Pharm. Pharm. Sci.* **6**:334–344 (2003).
 36. R. Bodmeier and O. Paeratakul. Mechanical properties of dry and wet cellulosic and acrylic films prepared from aqueous colloidal polymer dispersions used in the coating of solid dosage forms. *Pharm. Res.* **11**:882–888 (1994).
 37. O. Olabisi, L. M. Robeson, and M. T. Shaw. *Polymer—Polymer Miscibility*. Academic Press, New York, 1979.
 38. P. Sakellariou and R. C. Rowe. Interactions in cellulose derivative films for oral drug delivery. *Prog. Polym. Sci.* **20**:889–942 (1995).
 39. M. Song, A. Hammiche, H. M. Pollock, D. J. Hourston, and M. Reading. Modulated differential scanning calorimetry: 4. Miscibility and glass transition behavior in poly (methylmethacrylate) and poly(epichlorohydrin) blends. *Polym.* **37**:5661–5665 (1996).
 40. N. Nyamweya and S. W. Hoag. Assessment of polymer-polymer interactions in blends of HPMC and film forming polymers by modulated temperature differential scanning calorimetry. *Pharm. Res.* **17**:625–631 (2000).
 41. R. E. Wetton, R. D. L. Marsh, and J. G. Van-de-Velde. Theory and application of dynamic mechanical thermal analysis. *Thermochim. Acta* **175**:1–11 (1991).
 42. Y. Nishio and R. S. Manley. Cellulose/poly(vinyl alcohol) blends prepared from solutions in N,N-dimethylacetamide-lithium chloride. *Macromolecules* **21**:1270–1277 (1988).
 43. J. S. Park, J. W. Park, and E. Ruckenstein. A dynamic mechanical and thermal analysis of unplasticized and plasticized poly(vinyl alcohol)/ methylcellulose blends. *J. Appl. Polym. Sci.* **80**:1825–1834 (2001).
 44. S. Honary and H. Orafi. The effect of different plasticizer molecular weights and concentrations on mechanical and thermo-mechanical properties of free films. *Drug Dev. Ind. Pharm.* **28**: 711–715 (2002).
 45. T. T. Kararli, J. B. Hurlbut, and T. E. Needham. Glass-rubber transitions of cellulosic polymers by dynamic mechanical analysis. *J. Pharm. Sci.* **79**:845–848 (1990).
 46. In T. Murayama (ed.). *Dynamic Mechanical Properties of Polymeric Materials. Material Science Monographs*, Vol. 1. Elsevier, Amsterdam, 1978.
 47. In L. E. Nielsen (ed.). *Mechanical Properties of Polymers and Composites*, Vol. 1. Marcel Dekker, New York, 1974, Chap. 4, pp. 131–232.
 48. R. F. Boyer. In E. Bear, S. V. Radcliffe (eds.), *Polymer Materials: Relationship between Structure and Mechanical Behavior*, American Society for Metals, Metals Park, OH, 1974, pp 227–368.
 49. R. Nair, N. Nyamweya, S. Gönen, L. J. Martínez-Miranda, and S. W. Hoag. Influence of various drugs on the glass transition temperature of poly(vinylpyrrolidone): a thermodynamic and spectroscopic investigation. *Int. J. Pharm.* **225**:83–96 (2001).
 50. Gordon and J. S. Taylor. Ideal copolymers and the second order transition of synthetic rubbers 1. Non-crystalline co-polymers. *J. Appl. Chem.* **2**:493–500 (1952).
 51. R. Simha and R. F. Boyer. On a general relation involving the glass temperatures and coefficients of expansion of polymers. *J. Chem. Phys.* **37**:1003–1007 (1962).
 52. A. Hale and H. E. Blair. Polymer blends and block copolymers. In E. A. Turi (ed.), *Thermal Characterization of Polymeric Materials*, 2nd edition. Academic Press, San Diego, 1997, pp. 745–886.
 53. L. S. Taylor and G. Zografi. Sugar-polymer hydrogen bond interactions in lyophilized amorphous mixtures. *J. Pharm. Sci.* **87**: 1615–1621 (1998).
 54. Y. Nishio, T. Haratani, and T. Takahashi. Miscibility and orientation behavior of poly(vinyl alcohol)/poly(vinyl pyrrolidone) blends. *J. Polym. Sci.: Part B: Polymer Physics* **28**:377–386 (1990).
 55. J. P. Dechesne, J. Vanderschueren, and F. Jaminet. Influence des plastifiants sur la température de transition vitreuse de filmogènes gastroresistants enterosolubles. *J. Pharm. Belg.* **39**:341–347 (1984).
 56. P. Sakellariou. Effect of polymer miscibility on surface enrichment in polymer blends. *Polym.* **34**:3408–3415 (1993).
 57. P. Sakellariou and R. C. Rowe. Phase-separation and morphology in ethylcellulose cellulose-acetate phthalate blends. *J. Appl. Polym. Sci.* **43**:845–855 (1991).
 58. J. W. Mauger. Experimental methods to evaluate diffusion coefficients and investigate transport processes of pharmaceutical in-

- terest. In: G. L. Amidon, P. I. Lee, and E. M. Topp (eds.), *Transport Processes in Pharmaceutical Systems*. Marcel Dekker, New York, 1999, pp. 87–107.
59. M. E. Aulton, M. H. Abdul Razzak, and J. E. Hogan. Mechanical properties of hydroxypropylmethylcellulose films derived from aqueous systems. Part 2. Influence of solid inclusions. *Drug Dev. Ind. Pharm.* **10**:541–561 (1984).
60. R. C. Rowe. The cracking of film coatings on film-coated tablets—a theoretical approach with practical implications. *J. Pharm. Pharmacol.* **323**:423–426 (1981).
61. R. C. Rowe. Defects in film-coated tablets: aetiology and solutions. In D. Granderton and T. M. Jones (eds.), *Advances in Pharmaceutical Sciences*, Vol. 6. Academic Press, London, 1992, pp. 65–100.
62. S. G. Croll. The origin of residual internal stress in solvent-cast thermoplastic coatings. *J. App. Pol. Sci.* **23**:847–858 (1979).
63. K. Sato. The internal stress of coating films. *Prog. Organ. Coating* **8**:143–160 (1980).
64. R. C. Rowe. Correlations between the in-situ performance of tablet film coating formulations based on hydroxypropyl methylcellulose and data obtained from the tensile testing of free films. *Acta Pharm. Technol.* **29**:205–207 (1983).
65. E. Okutgen, J. E. Hogan, and M. E. Aulton. Effects of tablet core dimensional instability on the generation of internal stresses within film coats. Part 3. Exposure to temperatures and relative humidities which mimic the film coating process. *Drug Dev. Ind. Pharm.* **17**:2005–2016 (1991).
66. M. Tarvainen, R. Sutinen, S. Peltonen, H. Mikkonen, J. Maunus, K. Vähä-Heikkilä, V. P. Lehto, and P. Paronen. Enhanced film-forming properties for ethyl cellulose and starch acetate using n-alkenyl succinic anhydrides as novel plasticizers. *Eur. J. Pharm. Sci.* **19**:363–371 (2003).
67. E. S. Barabas. Vinyl alkyl ether polymers. In H. F. Mark (ed.), *Encyclopedia of Polymer Science and Engineering*: Vol. 17. Wiley-Interscience, New York, 1989, pp. 198.
68. A. O. Okhamafe and P. York. Interaction phenomena in pharmaceutical film coatings and testing methods. *Int. J. Pharm.* **39**: 1–21 (1987).
69. G. W. Radebaugh, J. L. Murtha, T. N. Julian, and J. N. Bondi. Methods for evaluating the puncture and shear properties of pharmaceutical polymeric films. *Int. J. Pharm.* **45**:39–46 (1988).
70. C. Remunan-Lopez and R. Bodmeier. Mechanical water uptake and permeability properties of crosslinked chitosan glutamate and alginate films. *J. Control. Rel.* **44**:215–225 (1997).
71. F. W. Harris. Introduction to polymer chemistry. In *State of the Art III: Polymer Chemistry*, American Chemical Society, 1981, pp. 837–843.